Myofibroblast communication is controlled by intercellular mechanical coupling

Lysianne Follonier[1], Sébastien Schaub[2], Jean-Jacques Meister[1] and Boris Hinz[1,*]

[1]Laboratory of Cell Biophysics, Ecole Polytechnique Fédérale de Lausanne (EPFL), Bâtiment SG–AA-B143, Station 15, CH-1015 Lausanne, Switzerland
[2]CNRS-UMR 6543, Centre A. Lacassagne, 33 Avenue Valombrose, Nice 06189, France
*Author for correspondence (e-mail: boris.hinz@epfl.ch)

Accepted 13 July 2008
Journal of Cell Science 121, 3305-3316 Published by The Company of Biologists 2008
doi:10.1242/jcs.024521

Summary

Neoformation of intercellular adherens junctions accompanies the differentiation of fibroblasts into contractile myofibroblasts, a key event during development of fibrosis and in wound healing. We have previously shown that intercellular mechanical coupling of stress fibres via adherens junctions improves contraction of collagen gels by myofibroblasts. By assessing spontaneous intracellular Ca^{2+} oscillations, we here test whether adherens junctions mechanically coordinate myofibroblast activities. Periodic Ca^{2+} oscillations are synchronised between physically contacting myofibroblasts and become desynchronised upon dissociation of adherens junctions with function-blocking peptides. Similar uncoupling is obtained by inhibiting myofibroblast contraction using myosin inhibitors and by blocking mechanosensitive ion channels using Gd^{3+} and GSMTx4. By contrast, gap junction uncouplers do not affect myofibroblast coordination. We propose the following model of mechanical coupling for myofibroblasts: individual cell contraction is transmitted via adherens junctions and leads to the opening of mechanosensitive ion channels in adjacent cells. The resulting Ca^{2+} influx induces a contraction that can feed back on the first cell and/or stimulate other contacting cells. This mechanism could improve the remodelling of cell-dense tissue by coordinating the activity of myofibroblasts.

Supplementary material available online at
http://jcs.biologists.org/cgi/content/full/121/20/3305/DC1

Key words: Adherens junction, Gap junction, Calcium oscillations, Mechanotransduction, Wound healing

Introduction

During wound healing and tissue repair, fibroblasts acquire smooth muscle cell characteristics and differentiate into contractile myofibroblasts, which are key players in physiological and pathological tissue remodelling (Desmouliere et al., 2005; Hinz, 2007). The first phenotypic transition into so-called proto-myofibroblasts is characterised by neoformation of contractile β-cytoplasmic actin stress fibres and occurs in response to profibrotic cytokines and to altered properties of the extracellular matrix (ECM) (Tomasek et al., 2002). In the presence of the transforming growth factor TGFβ1 in a mechanically restrained environment, these cells express α-smooth muscle actin (α-SMA) de novo, which significantly increases their contractile activity and is a hallmark of the differentiated myofibroblast (Hinz et al., 2001a; Hinz and Gabbiani, 2003b). In a rat model of wound healing, protomyofibroblasts dominate the earlier phase of granulation tissue formation and ECM secretion, whereas differentiated myofibroblasts promote the later phase of wound contraction (Darby et al., 1990; Hinz et al., 2001b). Tissue-derived fibroblasts cultured on rigid tissue surfaces spontaneously acquire the protomyofibroblast cytoskeletal organisation and will here be referred to as fibroblasts when not expressing α-SMA. Here, we compare these α-SMA-negative fibroblasts with differentiated myofibroblasts that express α-SMA.

Myofibroblast differentiation is accompanied by the formation of cell-cell adherens junctions that intercellularly couple contractile stress fibres (Hinz and Gabbiani, 2003a; Hinz et al., 2004; Pittet et al., 2008). In the intracellular portion of adherens junctions, actin filament bundles associate with a protein complex that contains catenins and which mediates binding to the cytoplasmic tail of transmembrane cadherins (Gumbiner, 2005; Nagafuchi, 2001; Weis and Nelson, 2006; Wheelock and Johnson, 2003). Notably, cadherin expression changes from N-cadherin (cadherin-2 or CADH2) in cultured fibroblasts and in protomyofibroblasts of early wound granulation tissue to OB-cadherin (cadherin-11 or CAD11) expression in differentiated myofibroblasts in vivo and in vitro (Hinz et al., 2004). At the single molecule level, OB-cadherin promotes stronger adhesion than N-cadherin in living myofibroblasts (Pittet et al., 2008) and the high intracellular tension generated by α-SMA leads to development of larger and more stable adherens junctions (Hinz et al., 2004). Moreover, inhibition of OB-cadherin but not of N-cadherin reduces collagen gel contraction by myofibroblasts, suggesting specific implication of OB-cadherin-type adherens junctions in transmitting contractile forces between myofibroblasts (Hinz et al., 2004). In addition to mechanical adherens junctions, fibroblastic cells can communicate electrochemically via gap junctions. Gap junction formation was demonstrated at the ultrastructural level between wound granulation tissue myofibroblasts (Gabbiani et al., 1978) and has also been reported between dermal fibroblasts in vivo (Salomon et al., 1988) and in cultured fibroblasts from different origins (Gilula et al., 1972; Ko et al., 2000; Petridou and Masur, 1996). Gap junctions allow intercellular passage of small molecules and ions, such as Ca^{2+}, by forming channels composed of transmembrane connexins (Evans and Martin, 2002; Saez et al., 2003). Connexin 43 (Cx43 or CXA1) appears to be the predominant connexin in fibroblastic cells. Cx43 has been implicated in coordinating fibroblast tension production in granulation tissue (Moyer et al., 2002) and in collagen gels (Ehrlich et al., 2000) suggesting that both electrochemical and mechanical

Journal of Cell Science

cell coupling improve tissue remodelling. However, it remains to be investigated how mechanical and electrochemical coupling can contribute to coordinating myofibroblast and fibroblast activities, respectively.

Here, we evaluated the role of electrochemical and mechanical cell-cell junctions in coordinating spontaneous and periodic transient increases in the intracellular Ca^{2+} ($Ca^{2+}_{[i]}$) concentration (oscillations). Periodic $Ca^{2+}_{[i]}$ oscillations have been described in different fibroblasts in response to various stimuli (Corps et al., 1989; Diliberto et al., 1994; Harootunian et al., 1991; Liang et al., 2003; Ridefelt et al., 1995; Uhlen et al., 2006; Wu et al., 2004) but their coordination between myofibroblasts has not yet been evaluated. Comparison of cultured fibroblasts and myofibroblasts in our study demonstrates that fibroblasts predominantly exhibit electrochemical coupling via gap junctions, whereas mechanical adherens junctions coordinate $Ca^{2+}_{[i]}$ oscillations between myofibroblasts. Our results suggest that local contractile events, following single $Ca^{2+}_{[i]}$ transients, are transmitted via adherens junctions to adjacent myofibroblasts. This mechanically stimulates Ca^{2+} influx through mechanosensitive ion channels (MS channels). The resulting contraction will establish a mechanical feedback loop to the first cell and recruit other connected cells to the synchronised population. In vivo, coordination of myofibroblast contraction may improve remodelling of a highly cellular tissue and at the same time inform individual cells about the contractile state of their neighbours.

Results

$Ca^{2+}_{[i]}$ oscillations are coordinated between contacting myofibroblasts

We compared rat subcutaneous fibroblasts in standard culture, where ~90% of the cells are negative for the myofibroblast marker α-SMA, with fibroblasts that had been pretreated with TGFβ1 for 4 days, inducing myofibroblast differentiation in ~90% of the cells (Hinz et al., 2001a). To elucidate whether both cell types exhibited spontaneous $Ca^{2+}_{[i]}$ oscillations, we loaded myofibroblasts (Fig. 1A) and fibroblasts (Fig. 1E) with the Ca^{2+} indicator Fura-2 and plotted changes in the fluorescence ratio over a recording time of 5-30 minutes (Fig. 1B,F). By relating the percentage of oscillating cells to the total number of cells in all image fields, we found periodic $Ca^{2+}_{[i]}$ oscillations in 31±18% of all myofibroblasts (n_{cells}=193, n_{exp}=25) and in 29±16% of all fibroblasts (n_{cells}=184, n_{exp}=18); hence the probability for spontaneous $Ca^{2+}_{[i]}$ oscillations was similar in both cell types.

To then determine whether fibroblast-to-myofibroblast differentiation changes the period of Ca^{2+} oscillations, we detected the principal peak of frequency in the power spectrum of all recorded fluorescence ratios (supplementary material Fig. S1A). Statistical analysis of the obtained histograms (Fig. 1C,G) revealed shorter mean oscillation period in myofibroblasts of 57±26 seconds compared with 70±26 seconds in fibroblasts; this difference was significant (Table 1). Separate analysis of contacting (Fig. 1D,H, blue) and of isolated cells (Fig. 1D,H, red) revealed no significant influence of physical cell-cell contact on the period distributions of both cell types (Table 1). However, qualitative assessment of video sequences of oscillating cells in confluent culture indicated coordination of $Ca^{2+}_{[i]}$ oscillations between contacting myofibroblasts that was less obvious between contacting fibroblasts (supplementary material Movie 1). This observation was corroborated by comparing the Ca^{2+} fluorescence ratios over time. Physically contacting myofibroblasts exhibited synchronised Ca^{2+} fluorescence ratio peaks (Fig. 1A,B, cells 1-3), which were not observed in isolated myofibroblasts (Fig. 1A,B, cell 4) or fibroblasts in general (Fig. 1E,F, all cells).

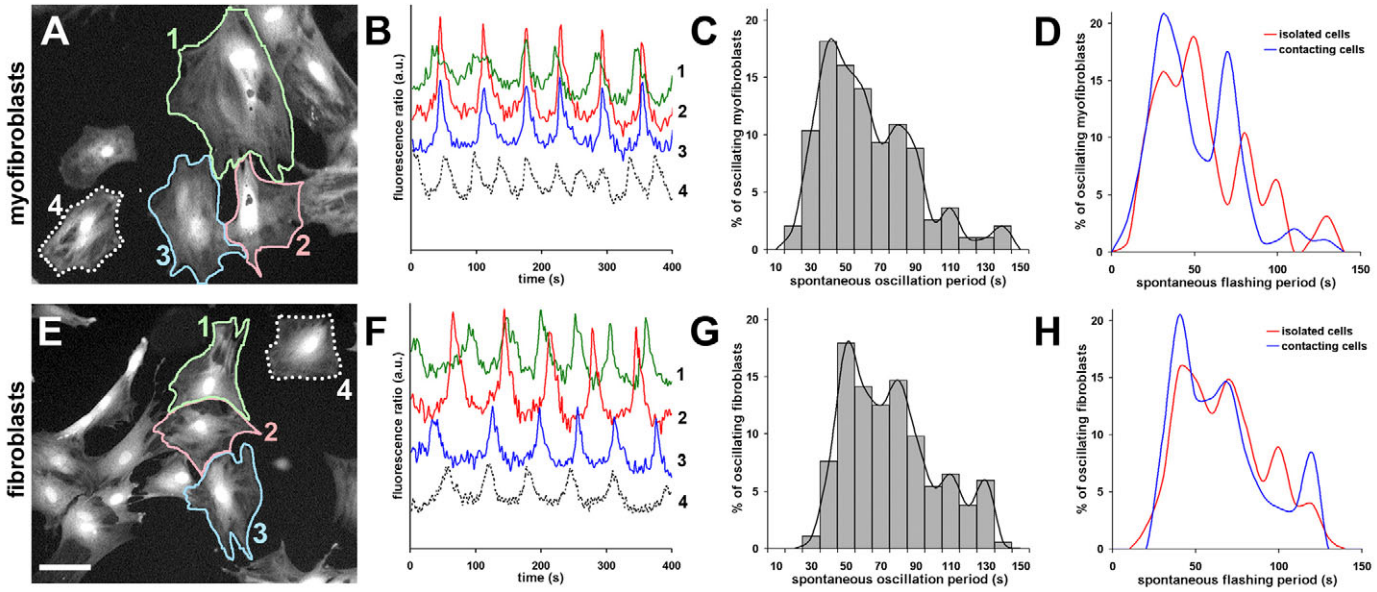

Fig. 1. Myofibroblasts and fibroblasts exhibit distinct periodic $Ca^{2+}_{[i]}$ oscillations. Spontaneous $Ca^{2+}_{[i]}$ oscillations in cultures of myofibroblasts (A-D) and of fibroblasts (E-H) (see also supplementary material Movie 1) were compared between contacting (continuous lines) and isolated cells (dotted lines). The Em_{340}/Em_{380} fluorescence ratios of Fura-2-loaded cells were recorded every 3-5 seconds over regions of interest including the entire cell (A and E show Em_{380} fluorescence image) and are plotted against time (B,F). The dominant periods of spontaneous $Ca^{2+}_{[i]}$ oscillations were determined by Fast Fourier Transform (Supplementary material Fig. S1A) of each profile and summarised in histograms for myofibroblasts (C, n_{exp}=25, n=193) and for fibroblasts (G, n_{exp}=18, n=184). (D,H) The dominant periods of $Ca^{2+}_{[i]}$ oscillations were separately analysed for contacting cell (blue histogram fit, myofibroblasts, n=97; fibroblasts, n=83) and isolated cells (red histogram fit, myofibroblasts, n=96; fibroblasts, n=101). This revealed no influence of the physical cell contact on the mean oscillation period within each group (Table 1). Scale bar: 50 μm.

Journal of Cell Science

Table 1. Statistical analysis of the influence of physical cell-cell contact on the period of spontaneous $Ca^{2+}_{[i]}$ oscillations in myofibroblasts and fibroblasts

Cell type	Condition	Mean	Median	s.d.	n_{cells}	n_{exp}
Myofibroblasts	Isolated	59	54	27	96	25
	Contacting	55	48	25	97	25
	All cells	57	51	26	193	25
Fibroblasts	Isolated	71	69	26	101	18
	Contacting	69	64	26	83	18
	All cells	70	67	26	184	18

The dominant $Ca^{2+}_{[i]}$ oscillation periods were determined by FFT for myofibroblasts and fibroblasts, either in physical contact, isolated or considering all cells. Respective mean and median values ± s.d. were determined and statistical differences are evaluated by calculating *P*-values, using a two-tailed heteroscedastic Student's *t*-test. Note that in all three sample populations, fibroblasts and myofibroblasts exhibit significantly different oscillation periods (isolated, $P>0.01$; contacting, $P<0.001$; all cells, $P<0.001$). The oscillation period is not significantly different when comparing isolated cells and cells in contact; $P>0.1$. n_{cells}, number of cells; n_{exp}, number of experiments.

To quantify the degree of cell-cell coordination, we compared cell pairs for the evolution of their oscillation periods over time (Fig. 2). Using a completely automated analysis, the periods between all $Ca^{2+}_{[i]}$ peaks were: (1) determined for each cell over the whole observation time; (2) matched between both cells according to their position on the time scale (Fig. 2A, first match connected with green line); and (3) displayed in a period scatter plot to illustrate the degree of correlation between the periods of both cells (Fig. 2B). To represent two different experimental conditions in one scatter plot and to facilitate direct comparison, all the values for one condition were reported to one side of the diagonal (where the periods of both cells are equal) by plotting the longer period versus the shorter period (all points above the diagonal, as in Fig. 2B) or vice versa (all points below the diagonal). The mean value of all data points of two compared cells was represented by the centre of an ellipse whose semi-major and semi-minor axes indicate standard deviation (s.d.) of the mean (Fig. 2B). Small ellipses and data point clouds close to the diagonal indicate high coordination of $Ca^{2+}_{[i]}$ oscillations between two cells; uncoupled cells are characterised by large ellipses and data point clouds far from the diagonal. With our method we were able to detect cell-cell coordination when cells oscillated with variable periods over time but always coordinated, and when cells oscillated with the same period but with a shifted phase, in the extreme case leading to oscillations in antiphase (supplementary material Fig. S1). Analysis of computationally simulated fluorescence profiles further demonstrated the potential of our method to detect different degrees of cell coupling (supplementary material Fig. S2).

With this method, we first analysed all possible non-contacting cell-pair combinations per experiment in control medium and plotted the data of all experiments in the period scatter plot above the diagonal (Fig. 3). To account for similar and thus superimposing values, we used a colour-coded diagram in which red indicates the highest occurrence of a value and blue indicates lowest occurrence. Both non-contacting myofibroblasts (Fig. 3A) and fibroblasts (Fig. 3B) displayed high variances in period comparison, meaning that data points were distributed far from the diagonal. This suggests that paracrine communication does not contribute to coordinating $Ca^{2+}_{[i]}$ oscillations activities in a given cell population. By contrast, comparing below the diagonal only periods between physically contacting cells (Fig. 3), revealed lower variation and thus higher coordination of myofibroblasts (Fig. 3A) compared with fibroblasts (Fig. 3B). Two-tailed heteroscedastic Student's *t*-tests were performed with the deviations of period pairs from the diagonal (Fig. 3A yellow line) and with the relative deviations (Fig. 3A,B, dotted line) (see Materials and Methods). This analysis revealed statistically significant difference between contacting and non-contacting myofibroblasts. By contrast, the difference between contacting and non-contacting fibroblasts was not significant (Table 2), despite the seemingly higher degree of scattering above the diagonal (all non-contacting cell pairs) (Fig. 3B). This can be explained by the higher total number of data points obtained and displayed for non-contacting cell pairs (n=482) compared with contacting cell pairs (n=55) (Table 2). Hence, spontaneous oscillations are coordinated between contacting myofibroblasts but occur more randomly between fibroblasts.

Fibroblasts and myofibroblasts communicate through different types of junctions

We have recently shown that fibroblast-to-myofibroblast transition is characterised by development of mechanically resistant adherens junctions (Hinz et al., 2004; Pittet et al., 2008). However,

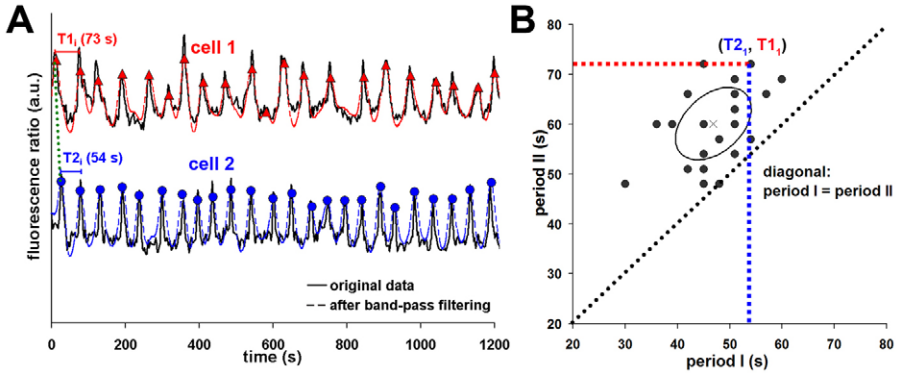

Fig. 2. Period comparison of cell pairs quantifies intercellular coupling. (A) To quantify intercellular coordination we compared over time the periods (defined as the time intervals between two consecutive $Ca^{2+}_{[i]}$ peaks) of cell pairs, here exemplified for two cells (cell 1, red; cell 2, blue). Fura-2 Em_{340}/Em_{380} fluorescence ratios (solid line) were band-pass filtered to eliminate noise (A, dashed lines) (supplementary material Fig. S1A, inset). First, all peaks (symbols) were automatically detected in the filtered curves, and the periods were determined. Second, over the whole observation time (here 1200 seconds), a computer algorithm matched for every peak i of cell 1 the closest peak on the time scale of cell 2 (first match connected with green dashed line). (B) Third, the periods $T1_i$ and $T2_i$ following these matched peaks are displayed in a scatter plot to illustrate the degree of correlation between these two variables. In such diagrams, every data point represents the matched periods of two cells at a given time point (first matched periods indicated with dotted lines). All values are reported to one side of the diagonal (where $T1_i$ equals $T2_i$) by plotting the longer period versus the shorter period (all points above the diagonal as in B) or vice versa (all points below the diagonal). This allows representation of two different experimental conditions in one scatter plot to facilitate direct comparison. The mean of all points ($T1_i$, $T2_i$) of two compared cells is represented by the centre of an ellipse of whose semi-major and semi-minor axes indicate s.d. The smaller the ellipse and the closer it is located with respect to the diagonal, the better the two cells are coordinated.

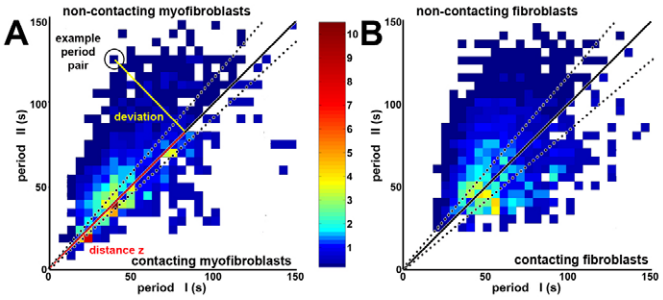

Fig. 3. $Ca^{2+}_{[i]}$ oscillations are coordinated between contacting myofibroblasts but random between fibroblasts and non-contacting cells. The periods between every two consecutive $Ca^{2+}_{[i]}$ peaks in the Fura-2 Em_{340}/Em_{380} fluorescence ratios of myofibroblasts (A) and fibroblasts (B) were compared over time for every possible cell pair combination within one image field (myofibroblasts, n_{exp}=25 and n_{cells}=193; fibroblasts, n_{exp}=18 and n_{cells}=184). All matching period pairs (square data points) obtained from cells that are not in physical contact are plotted as longer period versus shorter period above the diagonal (non-contacting pairs in myofibroblasts, *n*=324 and in fibroblasts, *n*=482). Period pairs obtained from all physically contacting cells are plotted as shorter period versus longer period below the diagonal (contacting pairs in myofibroblasts, *n*=60 and in fibroblasts, *n*=55). The occurrence of identical period pairs is colour-coded and normalised to the total number of data points in each condition (scale in %). The deviation of a period pair (one example encircled), i.e. its orthogonal distance to the diagonal, is demonstrated with a yellow line in A. By dividing the deviation by the distance *z* of the intersection point between the orthogonal and the diagonal to the origin (red section of diagonal) the relative deviation can be obtained (see Materials and Methods). The mean relative deviation is the average of all relative deviations and is represented as a dotted line.

myofibroblast differentiation in vivo is accompanied by decreased expression of the gap junction protein Cx43 (Mori et al., 2006). To investigate whether these different junction types contribute to the different degrees of intercellular Ca^{2+} coordination in cultured fibroblasts and myofibroblasts, we assessed formation of adherens junctions and gap junctions in both cell types by western blotting (Fig. 4A,B) and immunofluorescence (Fig. 4C,D) of the Triton-X-100-insoluble cytoskeleton fractions. Over 1-7 days of treatment with TGFβ1, fibroblasts increasingly expressed the myofibroblast marker α-SMA with maximum expression after 3 days, when they are considered to be myofibroblasts (Fig. 4A-C). Myofibroblasts show strong expression of β-catenin (Fig. 4A,B), which is the hallmark of large adherens junctions (Fig. 4C). By contrast, expression (Fig. 4A,B) and junctional localisation (Fig. 4C) of the gap junction marker Cx43 decreased by treatment with TGFβ1 (Fig. 4A) and was low in myofibroblasts (Fig. 4A-C). Inversely, fibroblasts exhibited strong staining and around three times higher expression of Cx43, and only punctuate staining and half the expression of β-catenin (Fig. 4A,B,D) compared with myofibroblasts.

To test whether Cx43-positive gap junctions were functional, we loaded cells with Lucifer Yellow (Fig. 5A-B,C, green) and neurobiotin (Fig. 5C, red), either by microinjecting individual cells in confluent monolayer (Fig. 5A,B) or by scrape-loading (Fig. 5C-E). Both methods demonstrated that the number of cell layers receiving small molecules via gap junction diffusion was low in myofibroblasts (Fig. 5C-E, Lucifer Yellow: 1.7±0.9; neurobiotin:

Table 2. Statistical evaluation of $Ca^{2+}_{[i]}$ oscillation coupling

A Condition	Cell	Contact	*n*	Mean T	*P*	Mean Rel. Dev. ± s.d.	*P*
Control	MF	+	60	8.4±12.5	<0.0001	0.071±0.09	<0.001
		–	324	16.5±14.8		0.137±0.10	
	F	+	55	19.9±16.8	n.s.	0.140±0.10	n.s.
		–	482	14.6±17.0		0.144±0.11	
B Inhibition	Cell	Drug	*n*	Mean T	*P*	Mean Rel. Dev. ± s.d.	*P*
Gap junctions	MF	Before	14	7.5±4.5	n.s.	0.079±0.05	n.s.
		After	14	8.7±7.0		0.095±0.07	
	F	Before	13	6.3±6.0	0.004	0.057±0.05	0.001
		After	13	20.4±19.1		0.129±0.10	
Adherens junctions	MF	Before	13	4.0±4.5	<0.0001	0.040±0.04	<0.001
		After	13	10.9±10.3		0.117±0.08	
	F	Before	10	4.0±4.7	n.s.	0.040±0.04	n.s.
		After	10	3.2±4.0		0.048±0.05	
Contraction	MF	Before	7	5.7±6.5	0.0002	0.049±0.05	<0.001
		After	7	13.5±11.3		0.115±0.09	
	F	Before	9	6.3±8.5	n.s.	0.066±0.07	n.s.
		After	9	7.5±5.9		0.079±0.06	
MS channels	MF	Before	14	7.6±5.8	0.0002	0.086±0.06	0.01
		After	14	18.5±13		0.140±0.10	
	F	Before	14	3.5±3.7	n.s.	0.041±0.04	n.s.
		After	14	4.0±5.3		0.044±0.05	

The table summarises the major statistical parameters that characterise the degree of $Ca^{2+}_{[i]}$ oscillation coupling between cell pairs. The mean of all period differences between cell pairs ΔT (ΔT = $|T1_i–T2_i|$) is reported in seconds ± s.d. Note that mean T values are generally small when cells are coupled and large when cell oscillations are not coordinated between cells. As a more stringent statistical criterion, means were calculated from the relative deviations [Rel. Dev. = $|T1_i–T2_i| / (T1_i+T2_i)$]. Statistical differences of the mean T values and of the mean relative deviations are evaluated by calculating *P*-values, using a two-tailed heteroscedastic Student's *t*-test. *n* indicates the number of cell pairs per group. Mean T and mean relative deviations of $Ca^{2+}_{[i]}$ oscillations are compared between physically contacting and non-contacting myofibroblasts (MF) and fibroblasts (F) in standard culture conditions (control). $Ca^{2+}_{[i]}$ oscillations coordination between contacting myofibroblasts is significantly different from that of non-contacting myofibroblast pairs. In addition, mean T and mean relative deviations are compared between fibroblastic cells before and after addition of various drugs. Note that only inhibition of gap junctions has a significant influence on fibroblast coupling, whereas myofibroblasts are significantly uncoupled upon inhibition of adherens junctions, cell contraction and MS channels. n.s. = non significant; *P*>0.1.

Journal of Cell Science

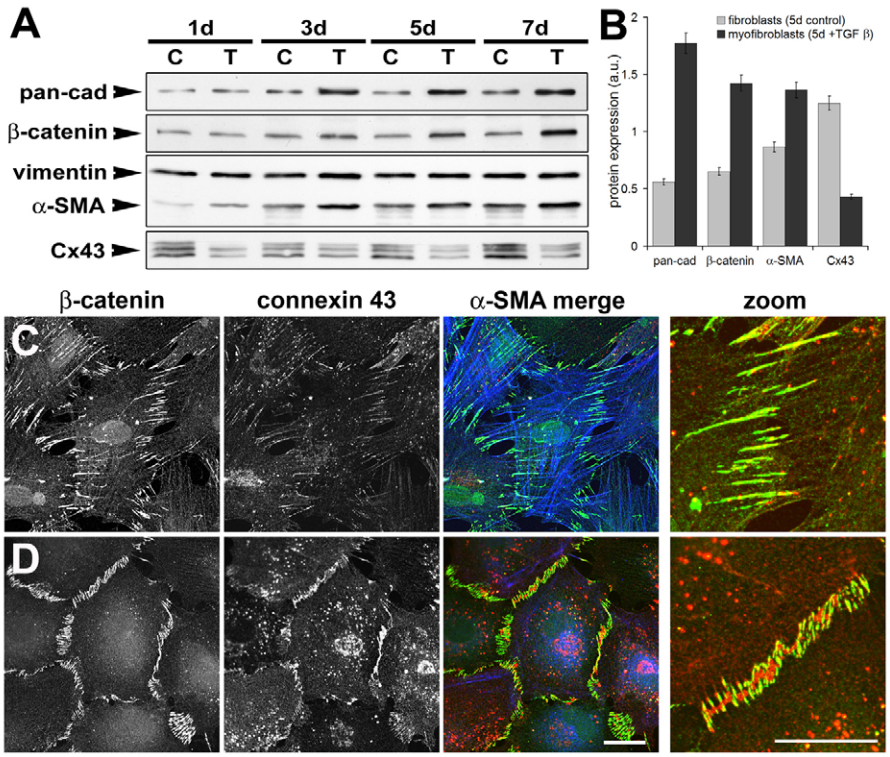

Fig. 4. Intercellular junctions differ between myofibroblasts and fibroblasts. (A) Expression of myofibroblast marker α-SMA, gap junction marker Cx43 and adherens junction markers pan-cadherin and β-catenin was assessed together with loading control vimentin, by western blotting. The cytoskeletal fractions are compared after 1-7 days culture between control fibroblasts (lanes labelled C) and fibroblasts treated with TGFβ1 to induce myofibroblast differentiation (lanes labelled T). (B) Band signal strength in western blots was analysed by optical densitometry and related to loading control vimentin (n=3). After 4 days of growth, Triton-X-100-extracted myofibroblasts (C) and fibroblasts (D) were immunostained for β-catenin (green), Cx43 (red) and α-SMA (blue). Scale bars, 25 μm.

2.3±1.0). Intercellular diffusion was around four times higher in fibroblasts (Fig. 5C-E, Lucifer Yellow: 6.9±1.7; neurobiotin: 10.3±1.5). This difference was similar using both small molecules despite the fact that neurobiotin diffused over ~1.4-times more cells than Lucifer Yellow (Fig. 5D,E). Treatment with palmitoleic acid and carbenoxolone, two well-accepted blocking agents of gap junction communication (Evans et al., 2006), strongly inhibited intercellular diffusion of small molecules in both cell types (Fig. 5C-E). These results show that myofibroblasts exhibit gap junction communication, which is however less prominent than that in fibroblasts.

To determine whether electrochemical communication contributes to the coordination of $Ca^{2+}_{[i]}$ oscillations between myofibroblasts, gap junctions were again uncoupled using palmitoleic acid (Fig. 6) and carbenoxolone (data not shown). In this and the following experiments (Fig. 7), we applied drugs during recording of Ca^{2+} oscillations of cell pairs that were preselected for synchronous oscillations in control conditions. This was particularly necessary for fibroblasts among which synchronously oscillating cells in contact represent only a minority of the population (c.f. Fig. 3). Nevertheless, $Ca^{2+}_{[i]}$ oscillations have been shown to be synchronised between fibroblasts that intrinsically oscillate with similar frequencies (Harks et al., 2003).

The coupled oscillation periods of contacting myofibroblasts remained unaltered despite gap junction uncoupling (Fig. 6A). The few contacting fibroblasts that were found to oscillate spontaneously in control conditions were desynchronised within 5 minutes after addition of palmitoleic acid (Fig. 6B, indicated by arrow length changes on top). To statistically evaluate the effect of palmitoleic acid on intercellular coordination, we summarised $Ca^{2+}_{[i]}$ oscillation periods for every pair of contacting cells in all experiments in one scatter plot (Fig. 6C,D). Data obtained in control conditions were displayed above the diagonal and period pairs obtained during palmitoleic acid treatment were plotted below the diagonal. All values obtained from one cell pair were represented by one distinct colour (Fig. 6C,D) and can thus be directly compared before and after drug treatment. Pairs of myofibroblasts exhibited coordinated oscillations and little variance before and after palmitoleic acid treatment and were thus largely independent from gap junction coupling (Fig. 6C). By contrast, intercellular coordination of fibroblast $Ca^{2+}_{[i]}$ oscillations strongly depended on electrochemical communication via gap junctions (Fig. 6D), indicated by significantly increased s.d. (larger ellipses), mean deviation and mean relative deviation (Table 2) after gap junction uncoupling.

Having shown that gap junction uncoupling has no effect on myofibroblast synchronisation, we elucidated the significance of mechanical intercellular coupling for myofibroblast communication. For this, we disassembled adherens junctions using a mix of peptides specifically directed against OB-cadherin and N-cadherin (Williams et al., 2000), the major cadherin types expressed in these cells (Hinz et al., 2004). We have previously shown that anti-N-cadherin and anti-OB-cadherin peptides efficiently inhibit formation of the respective cadherin junctions (Pittet et al., 2008) and disintegrate already existing adherens junctions in the same cell model (Hinz et al., 2004). We added anti-cadherin peptides for 45 minutes and assessed period coordination as described for gap junction uncoupling experiments. As before, we displayed periods of contacting cells above the diagonal before drug application and below the diagonal after drug treatment (Fig. 7). After inhibition of adherens junctions, previously coupled myofibroblasts lost their coordination as indicated by larger and more diagonal-distant ellipses (Fig. 7A; supplementary material Fig. S3A); this effect was significant (Table 2). By contrast, synchronised oscillations of pre-selected contacting fibroblasts remained coordinated and small ellipses remained close to the diagonal (Fig. 7B; supplementary material Fig. S3B), demonstrating that the used drugs had no

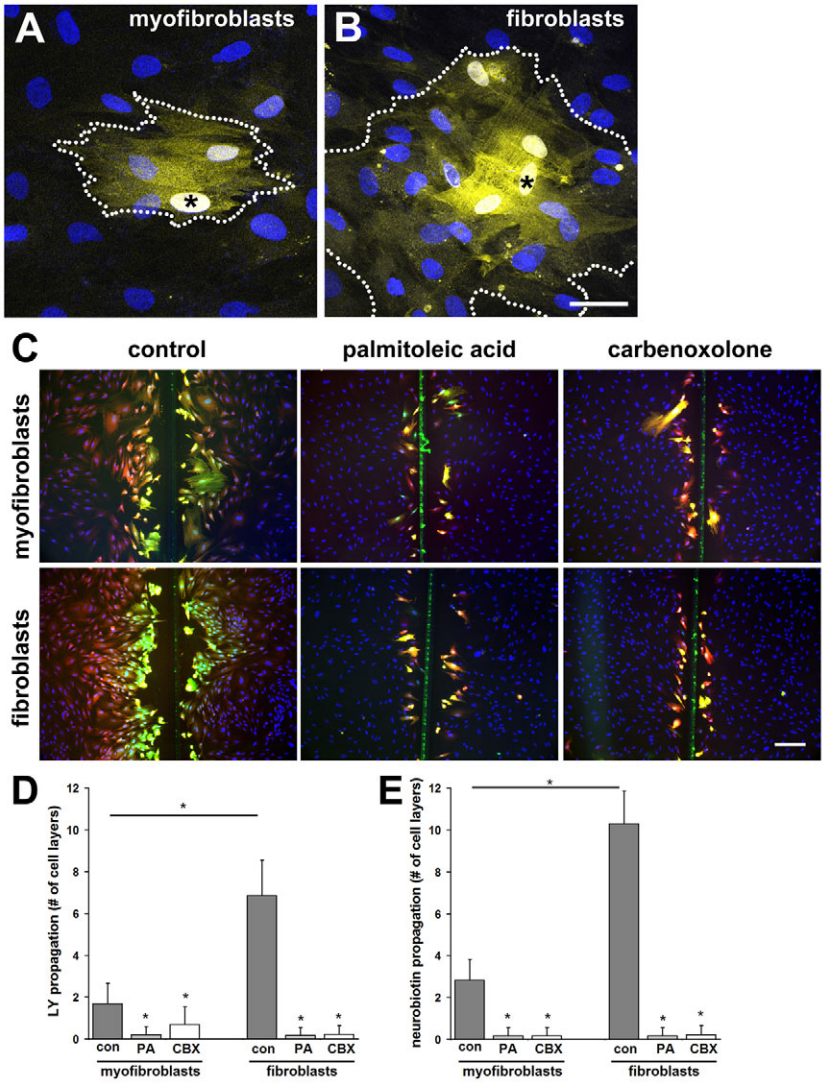

Fig. 5. Quantification of gap junction coupling by intercellular small molecule diffusion. To demonstrate gap junction coupling, individual myofibroblasts (A) and fibroblasts (B) in confluent monolayer were microinjected with Lucifer Yellow (yellow, *) and stained after diffusion for 5 minutes for cell nuclei (blue). Scale bar: 25 µm. (C) To quantify diffusion of small molecules through gap junctions, monolayers of myofibroblasts and fibroblasts were scrape-loaded with Lucifer Yellow (green) and neurobiotin (red) in control conditions (n=34) and in the presence of gap junction uncoupling agents palmitoleic acid (PA; n=11) and carbenoxolone (CBX; n=11). Scale bar: 100 µm. The number of cell layers receiving Lucifer Yellow (D) and neurobiotin (E) from the scrape wound was quantified; shown are means ±s.d. per experiment. *P≤0.001 compared with the respective control.

nonspecific effects. We conclude from these findings that mechanical coupling through adherens junctions plays a predominant role in coordinating myofibroblasts but not fibroblasts.

Myofibroblast communication implicates MS channels and transmission of cell contraction

One possibility of how stress-fibre-associated adherens junctions coordinate myofibroblast communication is that Ca^{2+}-induced contraction of one cell triggers a Ca^{2+} influx in the neighbouring cell by opening MS channels. Indeed, dramatic augmentation of the $Ca^{2+}_{[i]}$ by treating myofibroblasts with the Ca^{2+} ionophore A23187 resulted in visible cell contraction on wrinkling culture substrates within 10 minutes (see supplementary material Movie 2). It is conceivable that periodic $Ca^{2+}_{[i]}$ transients with smaller amplitude and duration induce small and short-lived contractile events that may not be resolvable with optical resolution. To test this hypothesis, we interfered with the actomyosin cytoskeleton by inhibiting cell contractile activity as well as by blocking MS channels during recording of $Ca^{2+}_{[i]}$ transients. Because all applied drugs caused an immediate change in $Ca^{2+}_{[i]}$ and briefly disturbed spontaneous $Ca^{2+}_{[i]}$ oscillations in individual cells, we compared cell-cell coordination 30 minutes after drug addition with the control; this was always sufficient to restore periodic $Ca^{2+}_{[i]}$ oscillations (Supplementary material Fig. S3C-F). Inhibition of cell contraction using 2,3-butanedione monoxime (BDM) (Fig. 7C,D; supplementary material Fig. S3C,D), blebbistatin and Y27632 (data not shown) significantly desynchronised contacting myofibroblasts (Fig. 7C; supplementary material Fig. S3C). The same drugs were almost without effect on the coordination of fibroblasts that have been preselected for synchronous oscillation (Fig. 7D; supplementary material Fig. S3D) (Table 2). This indicates that single-cell contraction is important in transmitting mechanical signals between myofibroblasts. Similarly, inhibition of MS channels with Gd^{3+} (Fig. 7E,F; supplementary material Fig. S3E,F) and with GSMTx4 (data not shown) significantly desynchronised $Ca^{2+}_{[i]}$ oscillations between contacting myofibroblasts (Fig. 7E; supplementary material Fig. S3E) but had little effect on fibroblasts (Fig. 7F; supplementary material Fig. S3F) (Table 2).

Intercellular propagation of $Ca^{2+}_{[i]}$ waves is delayed at myofibroblast junctions

Direct intercellular transmission of Ca^{2+} ions via gap junctions is only limited by diffusion and occurs with a velocity of ~30 µm/second (Sanderson et al., 1994). By contrast, our postulated mechanical trigger of $Ca^{2+}_{[i]}$ transients in myofibroblasts is indirect and should take longer because a contractile event and opening of MS channels need to precede the Ca^{2+} influx. To analyse the time course of $Ca^{2+}_{[i]}$ transient propagation, we grew myofibroblasts (Fig. 8A-C) and fibroblasts (Fig. 8D-F) in chains along microcontact-printed nonadhesive lines. This approach limited the number of possible partners to two cell neighbours, facilitating propagation analysis. A slow fluid flow applied perpendicularly to the lines excluded the possibility that propagation of single $Ca^{2+}_{[i]}$ transients (waves) was caused by cell-released and medium-diffusible factors. $Ca^{2+}_{[i]}$ transients were locally induced in individual cells and propagation of the induced $Ca^{2+}_{[i]}$ wave to adjacent cells was analysed with 1 frame/second time resolution. Mechanical stimulation with a micropipette and local application of Ca^{2+}/contraction-inducing agonists endothelin-1 and angiotensin-II all triggered $Ca^{2+}_{[i]}$ waves in fibroblasts and in myofibroblasts. Locally induced $Ca^{2+}_{[i]}$ waves propagated over up to six physically contacting cells with decreasing amplitude (Fig.

8B,E; supplementary material Movie 3); waves did not spread to cells grown on adjacent lines (Fig. 8B,E). Notably, propagation of a $Ca^{2+}_{[i]}$ waves over intercellular junctions was slower in myofibroblasts (Fig. 8B) than in fibroblasts (Fig. 8E, indicated by arrows). Kymograph analysis of Ca^{2+} fluorescence ratio values recorded along a line positioned over the cell chain confirmed that $Ca^{2+}_{[i]}$ waves propagated with a distinct intercellular delay that always occurred at the contact region between myofibroblasts (Fig. 8B). In the kymograph image, each delay appeared as a clear step along the time axis (*t*), which was hardly detectable between fibroblasts (Fig. 8E). Statistical analysis of such pausing events demonstrated that $Ca^{2+}_{[i]}$ wave propagation had an average delay of 6.2±3.0 seconds between myofibroblasts (Fig. 8C), which was three times shorter (2.7±1.6 seconds) between fibroblasts (Fig. 8F); this difference was statistically significant ($P<0.001$). When analysing $Ca^{2+}_{[i]}$ wave transmission over several cells, we determined a $Ca^{2+}_{[i]}$ wave propagation speed of 7.4±2.6 μm/second over myofibroblasts and 31.1±8.3 μm/second over fibroblasts. This difference was caused by the intercellular delay, because intracellular $Ca^{2+}_{[i]}$ wave propagation was similar in both cell types (~32 μm/second). The delayed transmission of $Ca^{2+}_{[i]}$ waves at intercellular junctions of myofibroblasts suggests a slower, potentially more complex mechanism of signal transmission compared with the faster signal propagation over several fibroblasts.

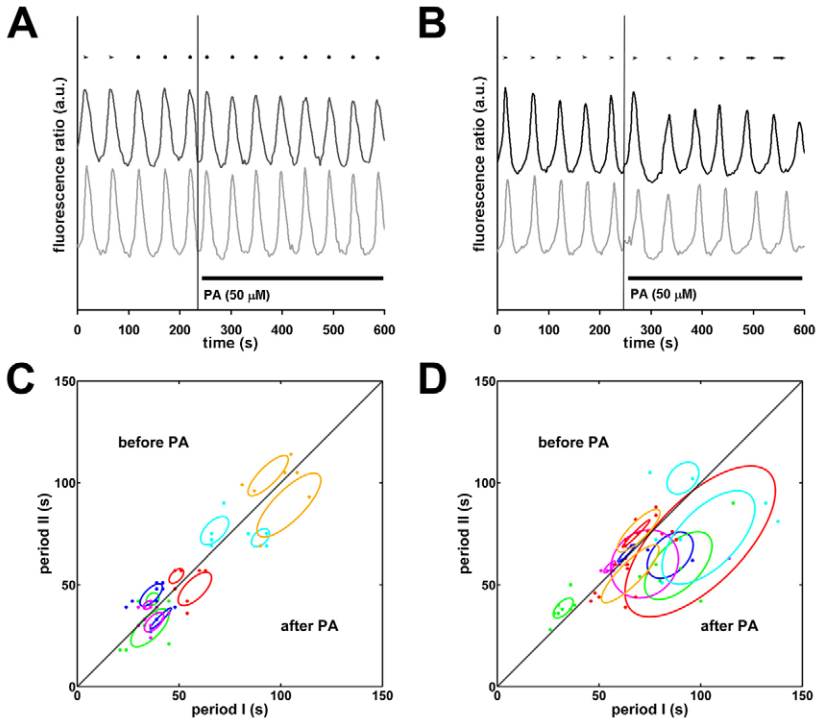

Fig. 6. Synchronisation of periodic $Ca^{2+}_{[i]}$ oscillations between fibroblasts is mediated by gap junction coupling. Spontaneous $Ca^{2+}_{[i]}$ oscillations in cultures of Fura-2-loaded myofibroblasts (A,C) and fibroblasts (B,D) were compared between contacting cells that were preselected for exhibiting coordinated periods. (A-B) Fura-2 Em_{340}/Em_{380} ratios were recorded every 3 seconds over regions of interest including the entire cell and are here displayed for two contacting cells. During recording, gap junctions were uncoupled by adding 50 μM palmitoleic acid (PA) at the indicated time point. Arrows on top of the fluorescence profiles indicate how the position of $Ca^{2+}_{[i]}$ peaks of cell 2 (grey) develops over time in respect to the matched peak of cell 1 (black); dots indicate simultaneous oscillations of both cells and changing arrow lengths over time demonstrate desynchronisation of the two cells. (C,D) For statistical analysis, all matched period pairs obtained before addition of palmitoleic acid are displayed as longer period versus shorter period (above diagonal) and all data obtained after palmitoleic acid treatment are plotted as shorter period versus longer period (below diagonal). The mean of all period pairs obtained from two contacting cells is represented by the centre of an ellipse of which semi-major and semi-minor axes indicate s.d. Each cell pair is represented by one colour. Note that ellipses become larger and more distant from the diagonal in fibroblasts after gap junction inhibition, indicating uncoupling of $Ca^{2+}_{[i]}$ oscillations.

Discussion

During development of fibrosis and during wound healing, fibroblasts develop a contractile apparatus that shares similarities with smooth muscle, highlighted by neoexpression of α-SMA (Hinz, 2007). Myofibroblast differentiation is further associated with the initiation and maturation of intercellular adherens junctions; the molecular composition of myofibroblast adherens junctions is beginning to be understood (Hinz et al., 2004) but their physiological function is still unknown. Here, we tested the hypothesis that adherens junctions coordinate the activity of contacting myofibroblasts. This coordination would gain importance during tissue remodelling when a high number of myofibroblasts contract the ECM at the same time.

Using spontaneous and periodic $Ca^{2+}_{[i]}$ oscillations as an indicator, we show that adherens junctions but not gap junctions synchronise the activity of cultured myofibroblasts. Because this function requires a functional actin cytoskeleton, cell contraction and MS channels, we propose the following model of intercellular mechanical coupling (Fig. 9A): the Ca^{2+}-induced contraction of one myofibroblast is transmitted to the contacting cell at sites of adherens junctions (Fig. 9B) and the resulting opening of MS channels leads to a Ca^{2+} rise in the second cell. The following contractile event can feed back to the first cell to maintain strong coordination (Fig. 9C) and can recruit other contacting cells to the synchronised population. Our simplified model demonstrates this coordination for a pair of myofibroblasts that in the extreme case display alternating oscillations; the model does not consider refractory phases of the involved channels that may account for more complex coordination pattern. Our $Ca^{2+}_{[i]}$ wave propagation experiments demonstrate that this model can be extended to Ca^{2+} transmission over small groups of cells.

One possibility to demonstrate different types of cell coupling is to analyse the intercellular propagation speed and travelling distance of $Ca^{2+}_{[i]}$ waves. $Ca^{2+}_{[i]}$ waves are triggered by local cell stimulation and then propagate intercellularly in cultures of normal rat kidney, subepithelial and ligament fibroblasts (De Roos et al., 1997; Furuya et al., 2005; Jones et al., 2005). When $Ca^{2+}_{[i]}$ transients take the form of action potentials, signals can propagate with a speed of several millimetres per second in fibroblasts; this fast electrical transmission involves gap junctions but not intercellular Ca^{2+} diffusion (Gaudesius et al., 2003; Harks et al., 2003). By contrast, Ca^{2+} signal propagation speed in our fibroblasts is several orders of magnitude slower (~30 μm/second). This is consistent with the velocity of $Ca^{2+}_{[i]}$ wave propagation between epithelial and glial cells (10-30 μm/second) over

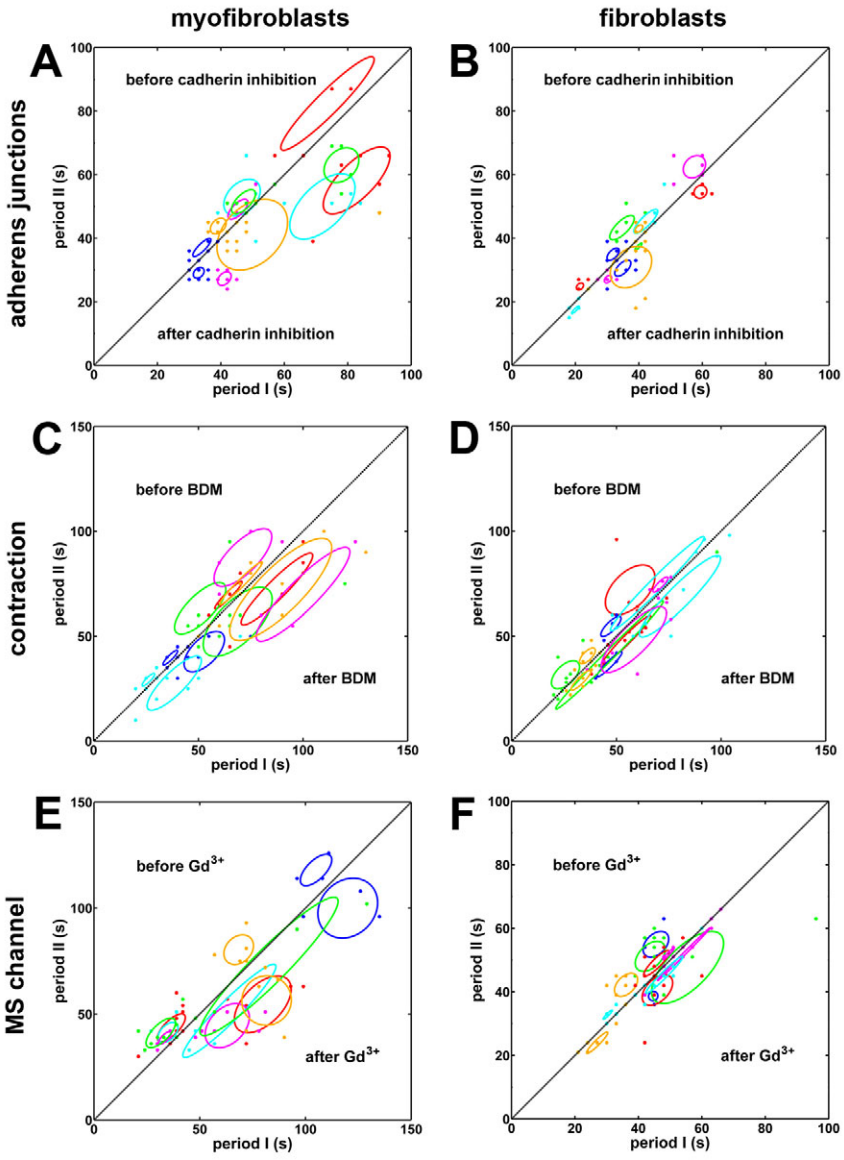

Fig. 7. Synchronisation of periodic $Ca^{2+}_{[i]}$ oscillations between myofibroblasts implies adherens junction coupling, cell contraction and MS channels. Spontaneous $Ca^{2+}_{[i]}$ oscillations in cultures of Fura-2-loaded myofibroblasts (A,C,E) and fibroblasts (B,D,F) were compared between contacting cells that were preselected for exhibiting coordinated periods. The corresponding Fura-2 Em_{340}/Em_{380} ratios of two contacting cells are shown in supplementary material Fig. S3. (A,B) adherens junctions were disassembled by adding a mixture of anti-N- and anti-OB-cadherin peptides at 0.5 mg/ml for 45 minutes. (C,D) Cell contraction was inhibited by adding 1 mM BDM. (E,F) MS channels were inhibited by adding 300 μM Gd^{3+}. All matched period pairs are reported above the diagonal before addition of the drug and below the diagonal after addition of the drug. The mean of all period pairs obtained from two contacting cells is represented by the centre of an ellipse of which semi-major and semi-minor axes indicate s.d.; each cell pair is represented by one colour. Note that ellipses become larger and more distant from the diagonal in myofibroblasts upon drug treatment, indicating uncoupling of $Ca^{2+}_{[i]}$ oscillations after inhibition of adherens junctions, of contraction and of MS channels.

short distances of several tens of micrometers (Sanderson et al., 1994). Such electrochemical transmission is rate limited by the diffusion of second messengers such as Ca^{2+} or inositol 1,4,5-trisphosphate through gap junctions.

Intercellular $Ca^{2+}_{[i]}$ wave propagation, triggered by local stimulation, follows different kinetics in cultured myofibroblasts compared with that in fibroblasts. Between myofibroblasts, $Ca^{2+}_{[i]}$ wave transmission is delayed at the junction for ~6 seconds; the delay was three times shorter in fibroblasts. One possibility is that this delay in the intercellular Ca^{2+} signal transmission between myofibroblasts is paracrine communication, which has been described for subepithelial fibroblasts that extracellularly release and respond to ATP after mechanical stimulation (Furuya et al., 2005). We can here formally exclude the influence of secreted factors because myofibroblasts require physical contact for $Ca^{2+}_{[i]}$ wave propagation, which is, in addition, not affected by application of fluid counterflow.

Another possible approach to assess the degree and type of intercellular coupling is to analyse $Ca^{2+}_{[i]}$ oscillations; this method bears the advantage of not interfering with the spontaneous activity of the cells. Periodic $Ca^{2+}_{[i]}$ oscillations with a frequency comparable with our observations (10-30 mHz), have been reported in fibroblastic cells only in response to various stimuli (Corps et al., 1989; Diliberto et al., 1994; Harootunian et al., 1991; Liang et al., 2003; Ridefelt et al., 1995; Uhlen et al., 2006; Wu et al., 2004). Our experiments establish for the first time that both cultured fibroblasts and myofibroblasts exhibit spontaneous and highly periodic $Ca^{2+}_{[i]}$ oscillations, which occur with higher frequency in myofibroblasts. The physiological relevance of this higher frequency is not clear, but it may be related to the higher contractile activity characteristic of differentiated myofibroblasts. This is supported by the observation that the frequency of cell shape oscillations in suspended fibroblasts increases with increasing actomyosin contractility (Salbreux et al., 2007).

Our experiments demonstrated that gap junction uncoupling desynchronises $Ca^{2+}_{[i]}$ oscillations between fibroblasts that have been pre-selected for coordinated oscillations (Fig. 6). By contrast, intercellular coordination is poor when considering all contacting fibroblasts in a given population (Fig. 3). This can be explained by previous findings that gap junction electrochemical coupling synchronises periodic $Ca^{2+}_{[i]}$ oscillations between fibroblasts that intrinsically oscillate with similar frequencies, but not when frequencies are significantly different, as reported for normal rat kidney fibroblasts after stimulation with prostaglandin F2α (Harks et al., 2003). Unlike fibroblasts, contacting myofibroblasts exhibit significantly higher intercellular coordination that is not affected by gap junction uncoupling, suggesting a different and more effective coupling mechanism. Fibroblast-to-myofibroblast differentiation is characterised by reduced gap junction formation and communication in our culture conditions; in support of this, downregulation of Cx43 was recently shown to accelerate wound healing in vivo (Mori et al., 2006).

Journal of Cell Science

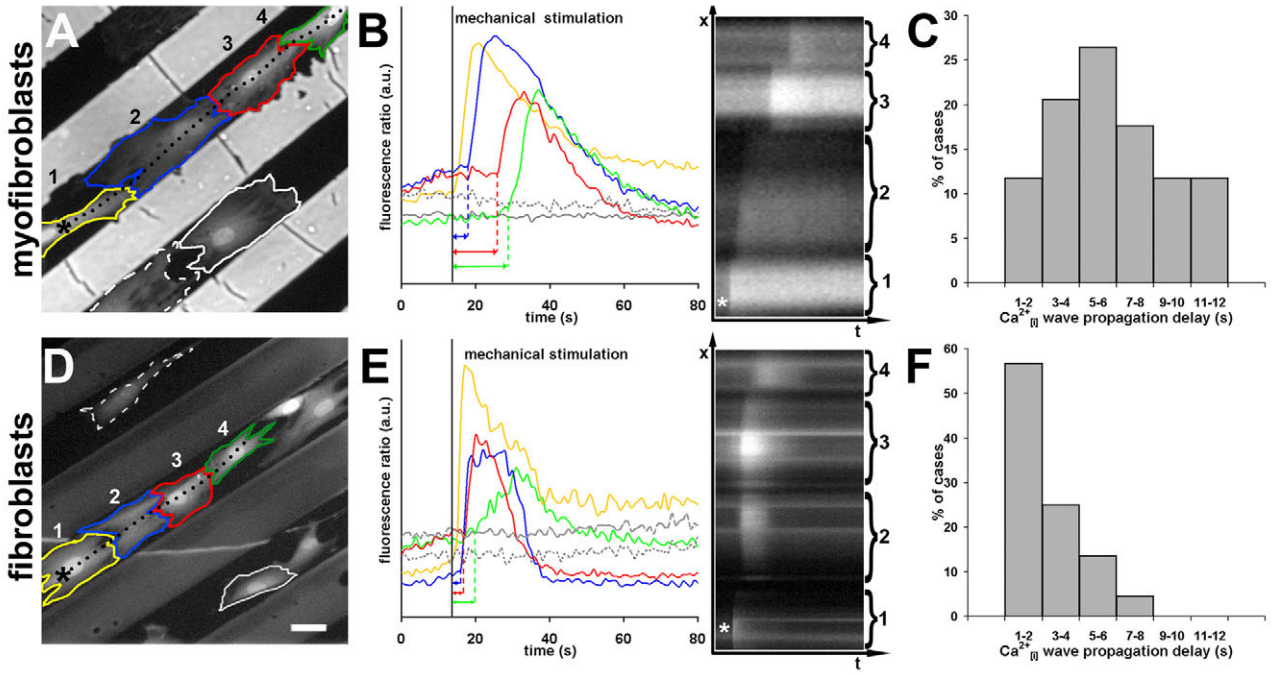

Fig. 8. Myofibroblasts and fibroblasts exhibit different kinetics of intercellular $Ca^{2+}_{[i]}$ wave propagation. Myofibroblasts (A-C) and fibroblasts (D-F) were grown between 50-µm-wide non-adhesive lines, created on glass by means of microcontact printing (A,D, Fura-2 Em_{380} fluorescence image, scale bar: 25 µm) (see also supplementary material Movie 3). Individual cells were locally stimulated by touching gently with a micropipette (*); $Ca^{2+}_{[i]}$ transients were analysed in the stimulated cell (yellow outline) and all following cells in the chain (blue to red to green; grey traces depict non-contacting control cells). Fura-2 Em_{340}/Em_{380} fluorescence ratios were recorded at 1 frame/second over the indicated cell outlines and plotted over time with the respective colour (B,E); arrows indicate time delay of $Ca^{2+}_{[i]}$ transient initiation after stimulation of the first cell (black line). A slow fluid flow applied perpendicularly to the lines excluded the possibility that released soluble factors induce a Ca^{2+} response. For quantitative analysis, fluorescence ratio intensity values were recorded along a line drawn across all cells in the chain (dotted line; A, 250 µm; D, 175 µm) and are displayed over time in a kymograph. In the kymograph image, delays of $Ca^{2+}_{[i]}$ wave propagation at cell junctions appear as clear steps along the time axis (t=40 seconds) in the case of myofibroblasts (B) but are hardly detectable between fibroblasts (E). All time delays at cell junctions were measured on kymograph images and summarised in histograms for myofibroblasts (C, n_{exp}=17, n_{pairs}=34) and for fibroblasts (F, n_{exp}=24, n_{pairs}=55).

Our data establish that myofibroblasts utilise a yet undiscovered mechanism of intercellular mechanical coupling via cadherins, which involves MS channels (Fig. 9). Specific disassembly of cadherin-containing adherens junctions, as well as blocking MS channels, both uncouple intercellularly coordinated $Ca^{2+}_{[i]}$ oscillations. Extracellular mechanical signals trigger $Ca^{2+}_{[i]}$ transients via MS channel opening (Zou et al., 2002), as demonstrated for fibroblasts after mechanical stimulation through cell-matrix integrin receptors (Glogauer et al., 1995; Hu et al., 2003; Munevar et al., 2004) as well as after cell stretching with micropipettes and stretchable culture substrates (Arora et al., 1994; Furuya et al., 2005). Similarly, mechanical stimulation with a blunt micropipette triggers a $Ca^{2+}_{[i]}$ wave in our myofibroblasts. Recently, MS channels were shown to associate with the actin cytoskeleton of endothelial cells at sites where stress fibres insert into cell adhesions (Hayakawa et al., 2008). This focusing of the Ca^{2+} entry to the adhesion sites can explain how a new Ca^{2+} wave is triggered at the cell-cell junction site upon stress fibre contraction in our experiments. Moreover, using cadherin-coated beads and micro-manipulated partner cells, McCulloch and co-workers have demonstrated that force applied via cadherin contacts triggers a Ca^{2+} response in fibroblastic cells, leading to local actin reorganisation (Chan et al., 2004; Ko et al., 2001a; Ko et al., 2001b). The authors proposed a model of cadherin-mediated mechanotransduction where actin-mediated reinforcement of adherens junctions represents a mechanoprotective response to high forces (Janmey and McCulloch, 2007; Ko and McCulloch, 2001).

We here add another physiological relevance to this model by proposing a Ca^{2+}-dependent mechanical communication between coupled myofibroblasts in which contraction of one cell mechanically triggers a $Ca^{2+}_{[i]}$ transient in its cadherin-coupled neighbour (Fig. 9). Consistently, inhibition of myofibroblast contraction abolishes intercellular synchronisation. To establish a mechanical feedback that can coordinate contacting cells, each single peak in the periodic $Ca^{2+}_{[i]}$ oscillations will evoke a contractile event (Fig. 9). Although such subcellular contractions were not directly observed in our experiments, myofibroblasts contract wrinkling silicone substrates when treated with Ca^{2+} ionophore and with contraction agonists that evoke $Ca^{2+}_{[i]}$ transients (Wipff et al., 2007). Moreover, high $Ca^{2+}_{[i]}$ concentration was shown to activate myosin light chain kinase via Ca^{2+}/calmodulin, leading to short-lived contraction similar to that in smooth muscle (Ehrlich et al., 1991; Katoh et al., 2001; Levinson et al., 2004). It is conceivable that contractions following $Ca^{2+}_{[i]}$ peaks in the oscillatory behaviour are locally restricted and too small to be detected with standard optical resolution. Indeed, stretches of below 1 µm, directly applied with a fibronectin-coated 10 µm bead to the membrane of endothelial cells, have been shown to elicit a Ca^{2+} response in the whole cell (Hayakawa et al., 2008). The corresponding force was estimated around 35 nN, which corresponds to the forces that are transmitted to single stress fibre attachment points, which can be either adherens junctions (Ganz et al., 2006) or focal adhesions (Balaban et al., 2001; Goffin et

Journal of Cell Science

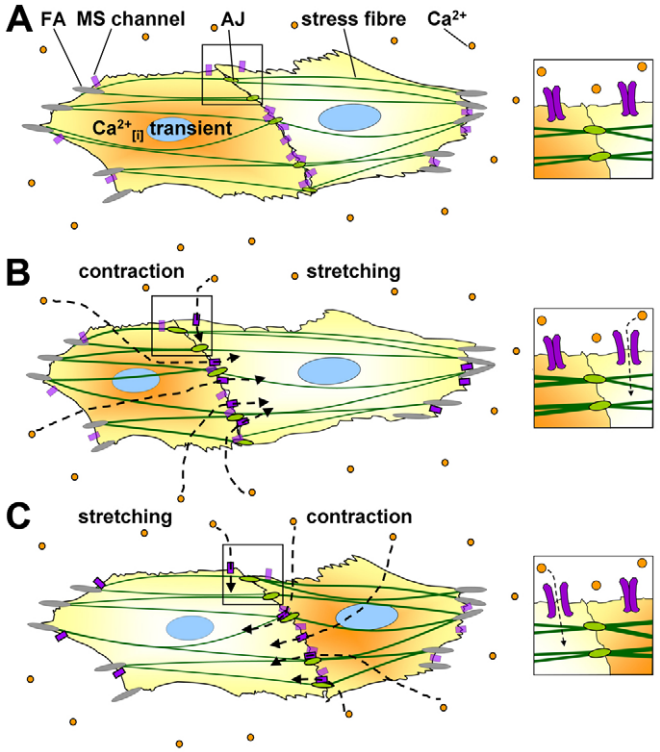

Fig. 9. Model of mechanical communication between contacting myofibroblasts. (A) The α-SMA-positive stress fibres (green) of contacting myofibroblasts are connected to the ECM at sites of focal adhesions (FA, grey) and intercellularly at sites of OB-cadherin-type adherens junctions (AJ; light green). MS channels (violet) in the plasma membrane are closed in relaxed cells (inset A) and do not permit entrance of Ca^{2+} ions (orange). Cytoskeleton-mediated or extracellular signalling events trigger a $Ca^{2+}_{[i]}$ transient (indicated by orange cytoplasm). (B) This rise in $Ca^{2+}_{[i]}$ leads to stress fibre contraction of the left cell (indicated by thicker fibres and cell shortening) that is transmitted to the right myofibroblast at sites of adherens junctions. The induced stretch leads to the opening of MS channels (inset B). (C) The resulting influx of Ca^{2+} through open MS channels then triggers a contractile event in the right cell that again feeds back to the left myofibroblast. At this point, the cycle can start again.

al., 2006). Moreover, culture on rigid substrates may damp visible overall cell contraction that is yet directly transmitted via adherens junctions between cells. Concomitantly, rhythmic contractions of 3T3 fibroblasts were shown to correlate with intrinsic periodic $Ca^{2+}_{[i]}$ oscillations under conditions of reduced substrate adhesion such as during spreading or in suspension (Pletjushkina et al., 2001; Salbreux et al., 2007).

How can periodic $Ca^{2+}_{[i]}$ oscillations contribute to tissue remodelling by myofibroblasts? At the tissue level, the development of persisting contractures by myofibroblast activity is a slow process that can last over several months or even years (Tomasek et al., 2002). We propose that periodic $Ca^{2+}_{[i]}$ oscillations at the cell level are associated with periodic microcontractile events that add up to overall tissue contraction. This implies a lock-step mechanism in which the locally contracted ECM is stabilised by addition of new ECM material. During the following relaxation and respreading of the cell, the ECM will remain shortened and many of these cycles will lead to incremental tissue contracture (Tomasek et al., 2002). This local mechanism is not captured by investigating tension development of myofibroblast-populated tissue strips and collagen gels in response to drug stimulation, which rather assesses the contractile force that is maximally developed by the whole cell population at one instant (Emmert et al., 2004; Hinz et al., 2001b; Kolodney et al., 1999; Nobe et al., 2003; Parizi et al., 2000; Tomasek et al., 2006). In addition, $Ca^{2+}_{[i]}$ oscillation-associated microcontractions may contribute to coordinating the activity of adjacent myofibroblasts that 'compete' for the same ECM during the remodelling process. We suggest that particularly strong adherens junctions mechanically couple the α-SMA-positive stress fibres of myofibroblasts to coordinate tension distribution within tissue under mechanical challenge, to propagate intracellular contraction signals and to synchronise myofibroblast contractile activity, therefore improving overall connective tissue remodelling.

Materials and Methods

Cell culture

Primary rat subcutaneous fibroblasts were obtained from explants and cultured up to passage seven in Dulbecco's modified Eagle's medium (DMEM) (Invitrogen, Basel, Switzerland), supplemented with 10% fetal calf serum (FCS) (BioConcept, Allschwil, Switzerland), 20 mM L-glutamine, and 1000 U/ml penicillin/streptomycin (Invitrogen). To induce myofibroblast differentiation, cells were treated for 4 days with 2 ng/ml TGFβ1 (Sigma, Buchs, Switzerland). For live videomicroscopy, cells were grown on home-made observation chambers with a glass coverslip bottom (#0) (Karl Hecht Assistent, Altnau, Switzerland), which were coated with 10 μg/ml collagen type I (Sigma), if not stated otherwise. In all experiments, fibroblasts were seeded at 4000 cells/cm^2 and cultured for 4 days.

Calcium imaging and image analysis

Cells in observation chambers were incubated for 1 hour at 37°C with 10 μM Fura-2 AM (Molecular Probes, Eugene, OR) in F-12 medium (Invitrogen) containing 10% FCS, 20 mM HEPES and 0.25% pluronic acid and subsequently washed for 30 minutes with F-12 containing 20 mM HEPES and 10% FCS. Ca^{2+} dynamics were observed using an inverted microscope (Axiovert S100TV, Carl Zeiss, Feldbach, Switzerland), equipped with a polychromatic Xenon light source (Polychrome IV, TILL Photonics, Ascheberg, Germany), high numerical aperture objectives (Fluar 10×, NA 0.5 and 20×, NA 0.75) (Carl Zeiss) and a charge-coupled device camera (C4742-95 Hamamatsu, Bucher Biotech, Basel, Switzerland). Samples were alternately excited at 340 nm and at 380 nm for 200 milliseconds; pairs of frames were recorded every 0.5-5 seconds using Openlab 3.0.6 software (Bucher Biotech). Increase in $Ca^{2+}_{[i]}$ leads to an increase in the emitted fluorescence at 510 nm after 340 nm excitation (Em_{340}) and decreasing emission after 380 nm excitation (Em_{380}). Changes in $Ca^{2+}_{[i]}$ levels over time were expressed in arbitrary units as $Ca^{2+}_{[i]}$ fluorescence ratio=Em_{340}/Em_{380}, calculated over regions of interest that included the entire cell (Metamorph, Universal Imaging, West Chester, PA).

Quantification of cell-cell coordination

Analysis of $Ca^{2+}_{[i]}$ oscillation coordination between cell pairs was performed with a completely automated computer algorithm, developed with Matlab 7.0 software (MathWorks, Natick, MA). First, the Ca^{2+} fluorescence ratios of two cells were plotted over time (Fig. 2A, continuous lines) and filtered with a frequency band pass (supplementary material Fig. S1A, inset) to eliminate noise (Fig. 2A, dashed lines). Second, the temporal position of every peak was determined by automatically localising the maxima of the filtered curves (Fig. 2A, filled symbols), and the periods were defined as the time intervals between two consecutive peaks. Third, for every peak i of cell 1 (Fig. 2A, red), the closest peak on the time scale of cell 2 (Fig. 2A, blue) was determined (Fig. 2A, dotted green line for first match). The corresponding periods $T1_i$ and $T2_i$ were then displayed in a period scatter plot (Fig. 2B, dotted lines indicate first match). The average of all points ($T1_i$, $T2_i$) was represented by the centre of an ellipse whose semi-major and semi-minor axes indicate s.d. of the mean (Fig. 2C). In such graphs, small ellipses and data point clouds close to the diagonal indicate high coordination of $Ca^{2+}_{[i]}$ oscillations between two cells.

Statistical analysis

Mean values are presented ± s.d. and tested by a two-tailed heteroscedastic Student's *t*-test. Differences were considered to be statistically significant when $P \leq 0.05$. 'Deviation' in period scatter plots is defined as the orthogonal distance (Fig. 3A, yellow line) between each data point ($T1_i$, $T2_i$) and the diagonal of the graph (period I=period II), i.e. deviation $= |T1_i - T2_i| / \sqrt{2}$. 'Relative deviation' is the deviation divided by the distance z of the intersection point between the orthogonal and the diagonal, to the origin (0, 0) (Fig. 3A, red section of diagonal), with $z = (T1_i + T2_i) / \sqrt{2}$, i.e. relative deviation $= |T1_i - T2_i| / (T1_i + T2_i)$. The larger the periods are, the greater is the deviation; hence the relative deviation accounts for this fact. 'Mean relative deviation' is the average of all relative deviations within one population (e.g. all contacting fibroblasts) and is used to characterise the degree of coordination of cell pairs within one population.

Journal of Cell Science

Cell stimulation and contraction analysis

The following drugs and agents were applied either to the experimental medium or locally in the vicinity of cells with the use of micropipettes and a micromanipulator (Leica, Heidelberg, Germany): BDM (1 mM), calcium ionophore A23187 (1 μM), carbenoxolone (100 μM), endothelin-1 (0.1 μM), Gd^{3+} (300 μM), palmitoleic acid (50 μM) (all Sigma), GSMTx4 (Peptides International, Louisville, KY) (5 μM), anti-N-cadherin (ADH126) (0.5 mg/ml), anti-OB-cadherin (ADH113) (0.5 mg/ml) (both Adherex Technologies, Research Triangle Park, Durham, NC), Y27632 (Calbiochem, San Diego, CA) (10 μM), angiotensin-II (Bachem, Bubendorf, Switzerland) (10 μM). To avoid diffusion of locally applied drugs or cell-secreted soluble factors, we performed selected experiments in a home-made open flow chamber with glass coverslip bottom. Flow (1 ml/minute) was created with a syringe pump (SP 210 IW, World Precision Instruments, Stevenage, UK); this slow flow rate did not stimulate cells mechanically and did not alter spontaneous $Ca^{2+}_{[i]}$ oscillations. Wrinkling silicone substrates to visualise cell contraction were prepared as described previously and surfaces were rendered adhesive for cell attachment by coating with collagen type I (10 μg/ml, Sigma) (Hinz et al., 2001a).

Microcontact printing and kymograph analysis

To facilitate observation of $Ca^{2+}_{[i]}$ wave propagation between fibroblasts and between myofibroblasts, cells were grown along straight lines of 50 μm width, created by a microcontact printing technique described previously (Goffin et al., 2006). Briefly, optical lithography was used to etch the topography of interest on a silicon wafer, serving as a mould to produce silicone stamps (Dow Corning, Wiesbaden, Germany). Stamps were cleaned with ethanol, treated for 30 seconds with plasma oxygen (Plasmaline, Tegal Corporation, Petaluma, CA) and incubated for 1 hour with comb polymer (a kind gift from A. Chilkoti, Duke University, Durham, NC) (Hyun and Chilkoti, 2001) (10 mg/ml in 50% ethanol). Conformal contact was made for 1 minute with the glass coverslip surface of observation chambers to transfer the protein- and cell-repellent polymer. Printed substrates were dried at 60°C overnight, immersed for 2 hours in water and then incubated with collagen type I (10 μg/ml) (Sigma). Fibroblasts adhered only between the comb-polymer-printed regions and were grown in line for 4 days with and without TGFβ1. Kymograph analysis (Hinz et al., 1999) was used to quantify the propagation speed of $Ca^{2+}_{[i]}$ waves between cells. Briefly, Em_{340} fluorescence values were recorded every second along a 10-pixel (5 μm)-wide line laid over several connecting cells and assembled as location (x) over time (t) in a kymograph image (Fig. 8).

Immunofluorescence, microscopy, antibodies and western blotting

To compare association of cell contact proteins with the cytoskeleton between both cell types, Triton-X-100-insoluble cytoskeletal protein fractions were obtained from cultured fibroblastic cells (Hinz et al., 2003). For immunofluorescence, cells were then fixed 10 minutes with 3% paraformaldehyde in PBS. As primary antibodies, we applied: anti-α-SMA (mouse IgG2a, SM-1, a kind gift from G. Gabbiani, University of Geneva, Switzerland) (Skalli et al., 1986), anti-β-catenin (rabbit, Zymed, Stehelin, Basel, Switzerland), anti-Cx43 (mouse IgG1, BD Biosciences, Allschwill, Switzerland) and anti-pan-cadherin (rabbit, Zymed). As secondary antibodies we applied: anti-mouse Alexa Fluor 568 and IgG2a Alexa Fluor 647, anti-rabbit Alexa Fluor 488 and Alexa Fluor 568 (all Molecular Probes), anti-mouse IgG2a-FITC, IgG1-TRITC and IgG1-FITC (all Southern Biotechnology, Birmingham, AL). Alexa Fluor 350-Phalloidin (Molecular Probes) was used to visualise F-actin and nuclei were stained with DAPI (Fluka, Buchs, Switzerland). Images were acquired using an oil-immersion objective 40×, NA 1.25 (Leica), mounted on an inverted confocal microscope (DM RXA2, with a laser-scanning confocal head TCS SP2 AOBS, Leica) and figures were assembled with Adobe Photoshop. Western blotting of Triton-X-100-insoluble cytoskeletal protein fractions was performed with the same primary antibodies, detected with HRP-conjugated secondary antibodies goat anti-mouse IgG and goat anti-rabbit IgG (Jackson ImmunoResearch Laboratories); equilibrated loading was tested by probing vimentin expression (clone V9, DAKO).

Cell loading with LY and neurobiotin

To quantify intercellular coupling via gap junctions, confluent cell monolayers were washed with Hank's buffered salt solution (HBSS) (Invitrogen) and then immersed with LY (Molecular Probes) (20 mg/ml) and neurobiotin (Vectorlabs, Burlingame, CA). The monolayer was then wounded with a cutter; for 5 minutes, wounded cells were allowed to absorb and to intercellularly transmit LY and neurobiotin, which are sufficiently small enough to propagate through gap junctions. Propagation was quantified by counting the number of cell layers that received small molecules from the wounded cells by intercellular diffusion. In another series of experiments, LY was injected into individual monolayer cells with a transjector (transjector 5246, Eppendorf, Schönenbuch, Switzerland) using micropipettes, produced from borosilicate glass capillaries (1.0 mm OD, 0.78 mm ID) (Harvard Apparatus, Les Ulis, France) with a micropipette puller (P-97 Brown-Flaming, Sutter Instrument Company, Novato, CA). Cells were then washed in HBSS, fixed for 10 minutes in 3% paraformaldehyde and stained for nuclei as described above. Neurobiotin was detected with Extravidin-TRITC (Sigma).

S. Bohnet and J. Goffin are gratefully acknowledged for expert help and J. Smith-Clerc for excellent technical assistance. We thank the staff of the The BioImaging and Optics platform of the Ecole Polytechnique Fédérale de Lausanne for providing image facilities and training. A. Chilkoti (Duke University, Durham, NC) is acknowledged for providing comb polymer and expert advice. Adherex Technologies (Research Triangle Park, Durham, NC) is acknowledged for providing high-quality anti-cadherin peptides. We thank James J. Tomasek for critically reading this manuscript. This work was supported by the Swiss National Science Foundation, grant 3100A0-102150/1 and by the Novartis Science Foundation.

References

Arora, P. D., Bibby, K. J. and McCulloch, C. A. (1994). Slow oscillations of free intracellular calcium ion concentration in human fibroblasts responding to mechanical stretch. *J. Cell Physiol.* **161**, 187-200.

Balaban, N. Q., Schwarz, U. S., Riveline, D., Goichberg, P., Tzur, G., Sabanay, I., Mahalu, D., Safran, S., Bershadsky, A., Addadi, L. et al. (2001). Force and focal adhesion assembly: a close relationship studied using elastic micropatterned substrates. *Nat. Cell Biol.* **3**, 466-472.

Chan, M. W., El Sayegh, T. Y., Arora, P. D., Laschinger, C. A., Overall, C. M., Morrison, C. and McCulloch, C. A. (2004). Regulation of intercellular adhesion strength in fibroblasts. *J. Biol. Chem.* **279**, 41047-41057.

Corps, A. N., Cheek, T. R., Moreton, R. B., Berridge, M. J. and Brown, K. D. (1989). Single-cell analysis of the mitogen-induced calcium responses of normal and protein kinase C-depleted Swiss 3T3 cells. *Cell Regul.* **1**, 75-86.

Darby, I., Skalli, O. and Gabbiani, G. (1990). Alpha-smooth muscle actin is transiently expressed by myofibroblasts during experimental wound healing. *Lab. Invest.* **63**, 21-29.

De Roos, A., Willems, P. H., van Zoelen, E. J. and Theuvenet, A. P. (1997). Synchronized Ca^{2+} signaling by intercellular propagation of Ca^{2+} action potentials in NRK fibroblasts. *Am. J. Physiol.* **273**, C1900-C1907.

Desmouliere, A., Chaponnier, C. and Gabbiani, G. (2005). Tissue repair, contraction, and the myofibroblast. *Wound Repair Regen.* **13**, 7-12.

Diliberto, P. A., Krishna, S., Kwon, S. and Herman, B. (1994). Isoform-specific induction of nuclear free calcium oscillations by platelet-derived growth factor. *J. Biol. Chem.* **269**, 26349-26357.

Ehrlich, H. P., Rockwell, W. B., Cornwell, T. L. and Rajaratnam, J. B. (1991). Demonstration of a direct role for myosin light chain kinase in fibroblast-populated collagen lattice contraction. *J. Cell Physiol.* **146**, 1-7.

Ehrlich, H. P., Gabbiani, G. and Meda, P. (2000). Cell coupling modulates the contraction of fibroblast-populated collagen lattices. *J. Cell Physiol.* **184**, 86-92.

Emmert, D. A., Fee, J. A., Goeckeler, Z. M., Grojean, J. M., Wakatsuki, T., Elson, E. L., Herring, B. P., Gallagher, P. J. and Wysolmerski, R. B. (2004). Rho-kinase-mediated Ca2+-independent contraction in rat embryo fibroblasts. *Am. J. Physiol. Cell Physiol.* **286**, C8-C21.

Evans, W. H. and Martin, P. E. (2002). Gap junctions: structure and function (Review). *Mol. Membr. Biol.* **19**, 121-136.

Evans, W. H., De Vuyst, E. and Leybaert, L. (2006). The gap junction cellular internet: connexin hemichannels enter the signalling limelight. *Biochem. J.* **397**, 1-14.

Furuya, K., Sokabe, M. and Furuya, S. (2005). Characteristics of subepithelial fibroblasts as a mechano-sensor in the intestine: cell-shape-dependent ATP release and P2Y1 signaling. *J. Cell Sci.* **118**, 3289-3304.

Gabbiani, G., Chaponnier, C. and Huttner, I. (1978). Cytoplasmic filaments and gap junctions in epithelial cells and myofibroblasts during wound healing. *J. Cell Biol.* **76**, 561-568.

Ganz, A., Lambert, M., Saez, A., Silberzan, P., Buguin, A., Mege, R. M. and Ladoux, B. (2006). Traction forces exerted through N-cadherin contacts. *Biol. Cell* **98**, 721-730.

Gaudesius, G., Miragoli, M., Thomas, S. P. and Rohr, S. (2003). Coupling of cardiac electrical activity over extended distances by fibroblasts of cardiac origin. *Circ. Res.* **93**, 421-428.

Gilula, N. B., Reeves, O. R. and Steinbach, A. (1972). Metabolic coupling, ionic coupling and cell contacts. *Nature* **235**, 262-265.

Glogauer, M., Ferrier, J. and McCulloch, C. A. (1995). Magnetic fields applied to collagen-coated ferric oxide beads induce stretch-activated Ca^{2+} flux in fibroblasts. *Am. J. Physiol.* **269**, C1093-C1104.

Goffin, J. M., Pittet, P., Csucs, G., Lussi, J. W., Meister, J. J. and Hinz, B. (2006). Focal adhesion size controls tension-dependent recruitment of alpha-smooth muscle actin to stress fibers. *J. Cell Biol.* **172**, 259-268.

Gumbiner, B. M. (2005). Regulation of cadherin-mediated adhesion in morphogenesis. *Nat. Rev. Mol. Cell. Biol.* **6**, 622-634.

Harks, E. G., Scheenen, W. J., Peters, P. H., van Zoelen, E. J. and Theuvenet, A. P. (2003). Prostaglandin F2 alpha induces unsynchronized intracellular calcium oscillations in monolayers of gap junctionally coupled NRK fibroblasts. *Pflugers Arch.* **447**, 78-86.

Harootunian, A. T., Kao, J. P., Paranjape, S. and Tsien, R. Y. (1991). Generation of calcium oscillations in fibroblasts by positive feedback between calcium and IP3. *Science* **251**, 75-78.

Hayakawa, K., Tatsumi, H. and Sokabe, M. (2008). Actin stress fibers transmit and focus force to activate mechanosensitive channels. *J. Cell Sci.* **121**, 496-503.

Hinz, B. (2007). Formation and function of the myofibroblast during tissue repair. *J. Invest. Dermatol.* **127**, 526-537.

Hinz, B. and Gabbiani, G. (2003a). Cell-matrix and cell-cell contacts of myofibroblasts: role in connective tissue remodeling. *Thromb. Haemost.* **90**, 993-1002.

Hinz, B. and Gabbiani, G. (2003b). Mechanisms of force generation and transmission by myofibroblasts. *Curr. Opin. Biotechnol.* **14**, 538-546.

Hinz, B., Alt, W., Johnen, C., Herzog, V. and Kaiser, H. W. (1999). Quantifying lamella dynamics of cultured cells by SACED, a new computer-assisted motion analysis. *Exp. Cell Res.* **251**, 234-243.

Hinz, B., Celetta, G., Tomasek, J. J., Gabbiani, G. and Chaponnier, C. (2001a). Alpha-smooth muscle actin expression upregulates fibroblast contractile activity. *Mol. Biol. Cell* **12**, 2730-2741.

Hinz, B., Mastrangelo, D., Iselin, C. E., Chaponnier, C. and Gabbiani, G. (2001b). Mechanical tension controls granulation tissue contractile activity and myofibroblast differentiation. *Am. J. Pathol.* **159**, 1009-1020.

Hinz, B., Dugina, V., Ballestrem, C., Wehrle-Haller, B. and Chaponnier, C. (2003). Alpha-smooth muscle actin Is crucial for focal adhesion maturation in myofibroblasts. *Mol. Biol. Cell* **14**, 2508-2519.

Hinz, B., Pittet, P., Smith-Clerc, J., Chaponnier, C. and Meister, J. J. (2004). Myofibroblast development is characterized by specific cell-cell adherens junctions. *Mol. Biol. Cell* **15**, 4310-4320.

Hu, S., Chen, J., Fabry, B., Numaguchi, Y., Gouldstone, A., Ingber, D. E., Fredberg, J. J., Butler, J. P. and Wang, N. (2003). Intracellular stress tomography reveals stress focusing and structural anisotropy in cytoskeleton of living cells. *Am. J. Physiol. Cell Physiol.* **285**, C1082-C1090.

Hyun, J. and Chilkoti, A. (2001). Micropatterning biological molecules on a polymer surface using elastomeric microwells. *J. Am. Chem. Soc.* **123**, 6943-6944.

Janmey, P. A. and McCulloch, C. A. (2007). Cell mechanics: integrating cell responses to mechanical stimuli. *Annu. Rev. Biomed. Eng.* **9**, 1-34.

Jones, B. F., Wall, M. E., Carroll, R. L., Washburn, S. and Banes, A. J. (2005). Ligament cells stretch-adapted on a microgrooved substrate increase intercellular communication in response to a mechanical stimulus. *J. Biomech.* **38**, 1653-1664.

Katoh, K., Kano, Y., Amano, M., Onishi, H., Kaibuchi, K. and Fujiwara, K. (2001). Rho-kinase-mediated contraction of isolated stress fibers. *J. Cell Biol.* **153**, 569-584.

Ko, K. S. and McCulloch, C. A. (2001). Intercellular mechanotransduction: cellular circuits that coordinate tissue responses to mechanical loading. *Biochem. Biophys. Res. Commun.* **285**, 1077-1083.

Ko, K., Arora, P., Lee, W. and McCulloch, C. (2000). Biochemical and functional characterization of intercellular adhesion and gap junctions in fibroblasts. *Am. J. Physiol. Cell Physiol.* **279**, C147-C157.

Ko, K. S., Arora, P. D., Bhide, V., Chen, A. and McCulloch, C. A. (2001a). Cell-cell adhesion in human fibroblasts requires calcium signaling. *J. Cell Sci.* **114**, 1155-1167.

Ko, K. S., Arora, P. D. and McCulloch, C. A. (2001b). Cadherins mediate intercellular mechanical signaling in fibroblasts by activation of stretch-sensitive calcium-permeable channels. *J. Biol. Chem.* **276**, 35967-35977.

Kolodney, M. S., Thimgan, M. S., Honda, H. M., Tsai, G. and Yee, H. F., Jr (1999). Ca^{2+}-independent myosin II phosphorylation and contraction in chicken embryo fibroblasts. *J. Physiol.* **515** (Pt 1), 87-92.

Levinson, H., Moyer, K. E., Saggers, G. C. and Ehrlich, H. P. (2004). Calmodulin-myosin light chain kinase inhibition changes fibroblast-populated collagen lattice contraction, cell migration, focal adhesion formation, and wound contraction. *Wound Repair Regen.* **12**, 505-511.

Liang, W., McDonald, P., McManus, B., van Breemen, C. and Wang, X. (2003). Histamine-induced Ca(2+) signaling in human valvular myofibroblasts. *J. Mol. Cell Cardiol.* **35**, 379-388.

Mori, R., Power, K. T., Wang, C. M., Martin, P. and Becker, D. L. (2006). Acute downregulation of connexin43 at wound sites leads to a reduced inflammatory response, enhanced keratinocyte proliferation and wound fibroblast migration. *J. Cell Sci.* **119**, 5193-5203.

Moyer, K. E., Davis, A., Saggers, G. C., Mackay, D. R. and Ehrlich, H. P. (2002). Wound healing: the role of gap junctional communication in rat granulation tissue maturation. *Exp. Mol. Pathol.* **72**, 10-16.

Munevar, S., Wang, Y. L. and Dembo, M. (2004). Regulation of mechanical interactions between fibroblasts and the substratum by stretch-activated Ca^{2+} entry. *J. Cell Sci.* **117**, 85-92.

Nagafuchi, A. (2001). Molecular architecture of adherens junctions. *Curr. Opin. Cell Biol.* **13**, 600-603.

Nobe, H., Nobe, K., Fazal, F., De Lanerolle, P. and Paul, R. J. (2003). Rho kinase mediates serum-induced contraction in fibroblast fibers independent of myosin LC20 phosphorylation. *Am. J. Physiol. Cell Physiol.* **284**, C599-C606.

Parizi, M., Howard, E. W. and Tomasek, J. J. (2000). Regulation of LPA-promoted myofibroblast contraction: role of Rho, myosin light chain kinase, and myosin light chain phosphatase. *Exp. Cell Res.* **254**, 210-220.

Petridou, S. and Masur, S. K. (1996). Immunodetection of connexins and cadherins in corneal fibroblasts and myofibroblasts. *Invest. Ophthalmol. Vis. Sci.* **37**, 1740-1748.

Pittet, P., Lee, K., Kulik, A. J., Meister, J. J. and Hinz, B. (2008). Fibrogenic fibroblasts increase intercellular adhesion strength by reinforcing individual OB-cadherin bonds. *J. Cell Sci.* **121**, 877-886.

Pletjushkina, O. J., Rajfur, Z., Pomorski, P., Oliver, T. N., Vasiliev, J. M. and Jacobson, K. A. (2001). Induction of cortical oscillations in spreading cells by depolymerization of microtubules. *Cell Motil. Cytoskeleton* **48**, 235-244.

Ridefelt, P., Yokote, K., Claesson-Welsh, L. and Siegbahn, A. (1995). PDGF-BB triggered cytoplasmic calcium responses in cells with endogenous or stably transfected PDGF beta-receptors. *Growth Factors* **12**, 191-201.

Saez, J. C., Berthoud, V. M., Branes, M. C., Martinez, A. D. and Beyer, E. C. (2003). Plasma membrane channels formed by connexins: their regulation and functions. *Physiol. Rev.* **83**, 1359-1400.

Salbreux, G., Joanny, J. F., Prost, J. and Pullarkat, P. (2007). Shape oscillations of non-adhering fibroblast cells. *Phys. Biol.* **4**, 268-284.

Salomon, D., Saurat, J. H. and Meda, P. (1988). Cell-to-cell communication within intact human skin. *J. Clin. Invest.* **82**, 248-254.

Sanderson, M. J., Charles, A. C., Boitano, S. and Dirksen, E. R. (1994). Mechanisms and function of intercellular calcium signaling. *Mol. Cell Endocrinol.* **98**, 173-187.

Skalli, O., Ropraz, P., Trzeciak, A., Benzonana, G., Gillessen, D. and Gabbiani, G. (1986). A monoclonal antibody against alpha-smooth muscle actin: a new probe for smooth muscle differentiation. *J. Cell Biol.* **103**, 2787-2796.

Tomasek, J. J., Gabbiani, G., Hinz, B., Chaponnier, C. and Brown, R. A. (2002). Myofibroblasts and mechano-regulation of connective tissue remodelling. *Nat. Rev. Mol. Cell. Biol.* **3**, 349-363.

Tomasek, J. J., Vaughan, M. B., Kropp, B. P., Gabbiani, G., Martin, M. D., Haaksma, C. J. and Hinz, B. (2006). Contraction of myofibroblasts in granulation tissue is dependent on Rho/Rho kinase/myosin light chain phosphatase activity. *Wound Repair Regen.* **14**, 313-320.

Uhlen, P., Burch, P. M., Zito, C. I., Estrada, M., Ehrlich, B. E. and Bennett, A. M. (2006). Gain-of-function/Noonan syndrome SHP-2/Ptpn11 mutants enhance calcium oscillations and impair NFAT signaling. *Proc. Natl. Acad. Sci. USA* **103**, 2160-2165.

Weis, W. I. and Nelson, W. J. (2006). Re-solving the cadherin-catenin-actin conundrum. *J. Biol. Chem.* **281**, 35593-35597.

Wheelock, M. J. and Johnson, K. R. (2003). Cadherins as modulators of cellular phenotype. *Annu. Rev. Cell Dev. Biol.* **19**, 207-235.

Williams, E., Williams, G., Gour, B. J., Blaschuk, O. W. and Doherty, P. (2000). A novel family of cyclic peptide antagonists suggests that N-cadherin specificity is determined by amino acids that flank the HAV motif. *J. Biol. Chem.* **275**, 4007-4012.

Wipff, P. J., Rifkin, D. B., Meister, J. J. and Hinz, B. (2007). Myofibroblast contraction activates latent TGF-beta1 from the extracellular matrix. *J. Cell Biol.* **179**, 1311-1323.

Wu, C., Sui, G. P. and Fry, C. H. (2004). Purinergic regulation of guinea pig suburothelial myofibroblasts. *J. Physiol.* **559**, 231-243.

Zou, H., Lifshitz, L. M., Tuft, R. A., Fogarty, K. E. and Singer, J. J. (2002). Visualization of Ca2+ entry through single stretch-activated cation channels. *Proc. Natl. Acad. Sci. USA* **99**, 6404-6409.

Journal of Cell Science